Supporting Information

Oil/water separation membranes with fluorine island structure for stable high flux

Mingrui He, Panpan Wang, Runnan Zhang, Zhongyi Jiang, Xu He, Jun Ma**

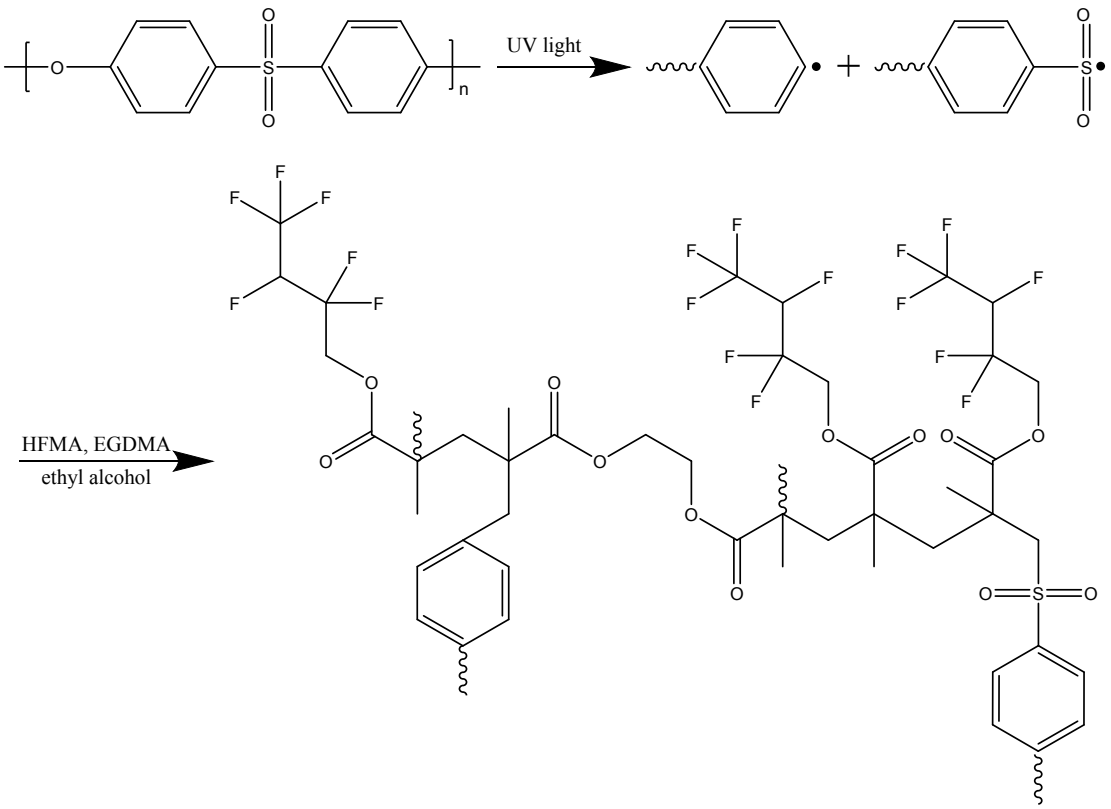

Fig. S1. Schematic diagram of the UV-induced grafting of fluoropolymer on the membrane surface.

Table S1. Tensile strength of the membranes

Membrane	Yield stress (MPa)	Yield strain (%)	Breaking stress (MPa)	Breaking strain (%)
NM	39.5±2.0	4.1±0.6	66.2±2.4	62.3±4.1
UM	40.2±1.4	4.2±0.9	65.9±3.6	62.9±6.5
M125	39.1±2.3	3.9±0.7	66.3±1.9	61.5±3.3
M450	38.9±2.6	4.1±0.2	66.7±2.4	62.7±5.6

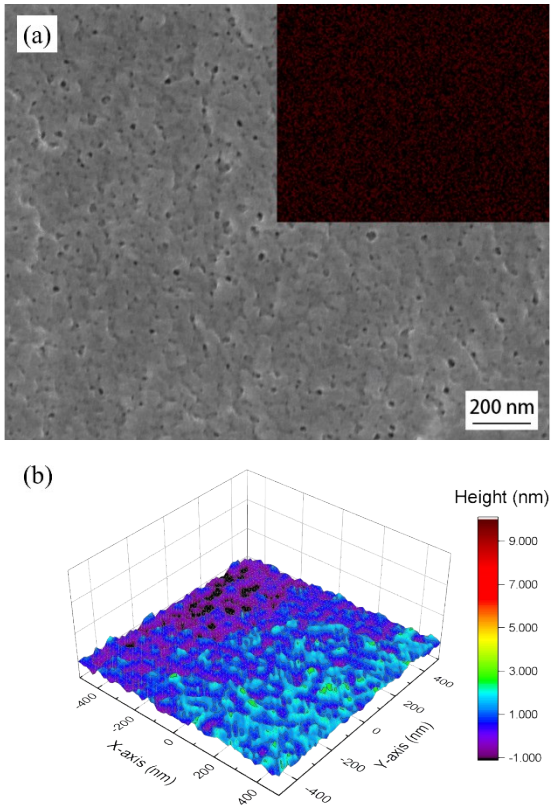

Fig. S2. Surface morphologies and chemical compositions of (a) the UM membrane observed by the SEM and the EDS. Surface topographies of (b) the UM membrane measured by the AFM.

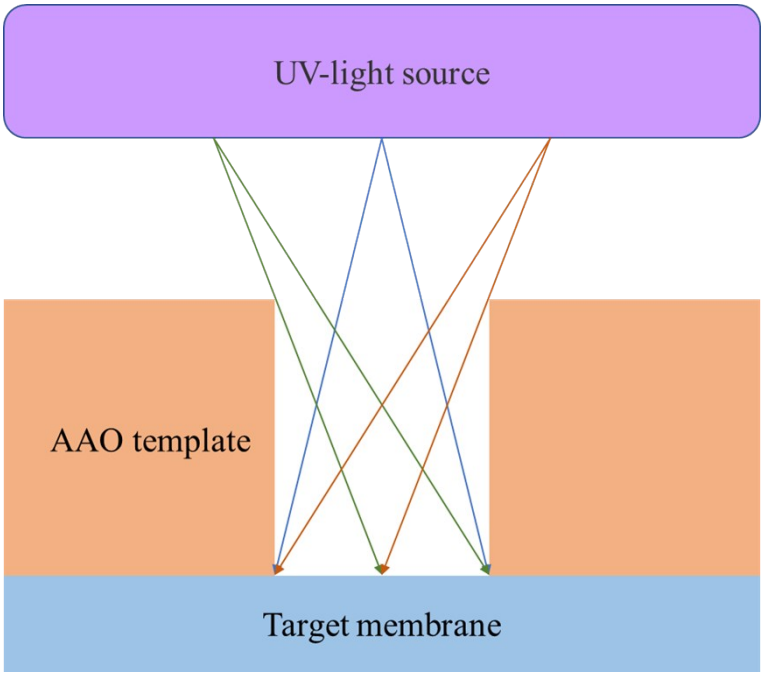

Fig. S3. Schematic illustration of the UV-light path through the hole of AAO tmeplate.

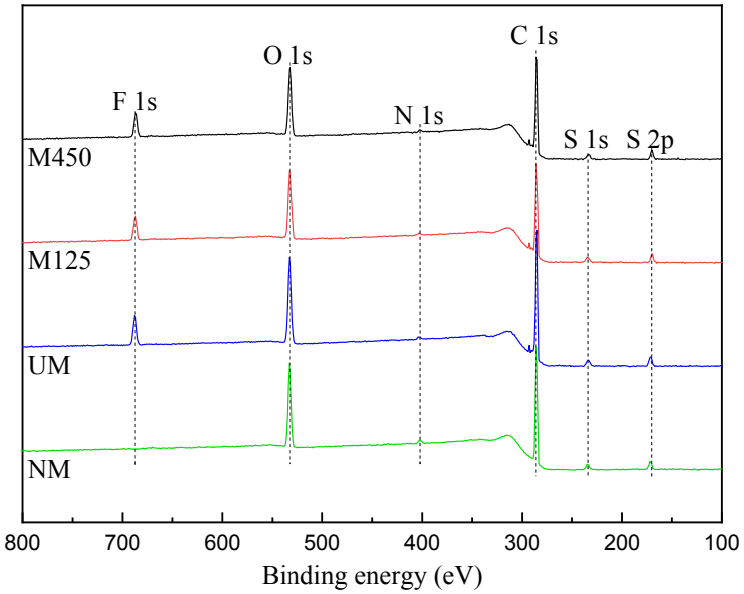

Fig. S4. XPS full spectrum of the membranes.

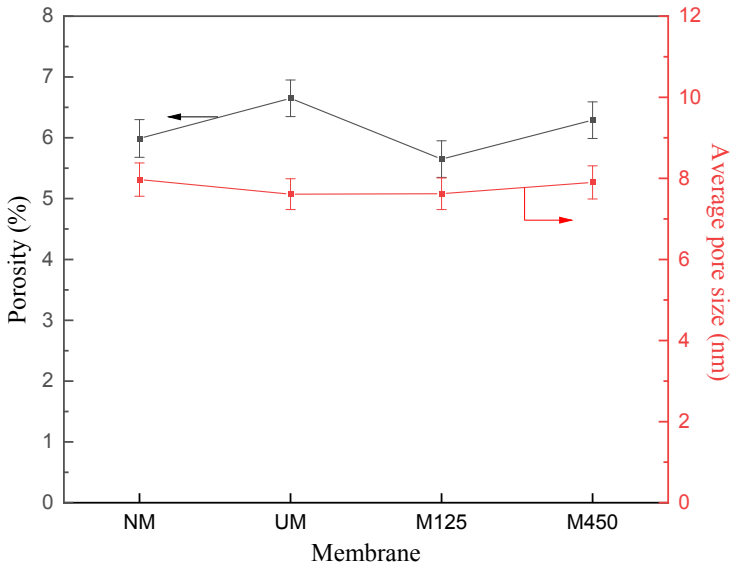

Fig. S5. Porosity and average pore sizes of the membranes.

Table S2. Advancing and receding water contact angles as well as surface free energy of the membranes.

Membrane	Surface free energy (mJ/m^2)			Dynamic water contact angle (^{o})		
	γ	γ	γ	θ_a	θ_r	$\Delta\theta$
NM	39	39	39	62.5	44.9	17.6
UM	18.7	18.7	18.7	93.7	41.3	52.4
M125	19.7	19.7	19.7	92.4	31.7	60.7
M450	19.3	19.3	19.3	92.5	29	63.5

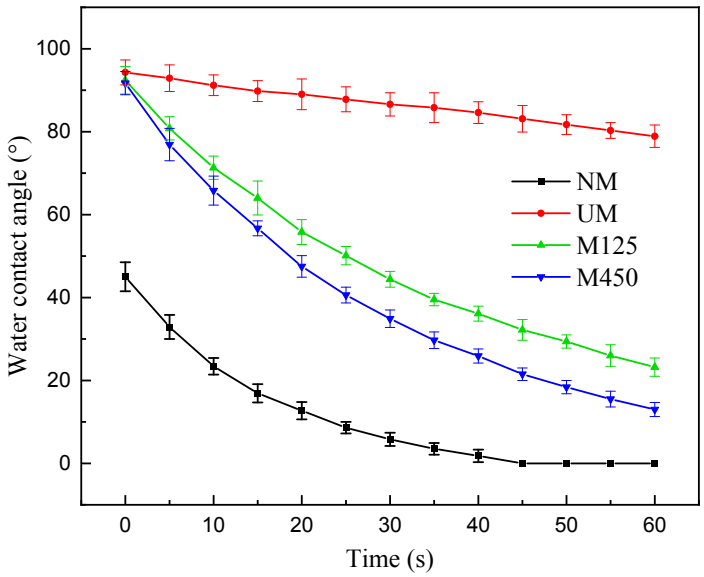

Fig. S6. Time-dependent water contact angles of the membranes.

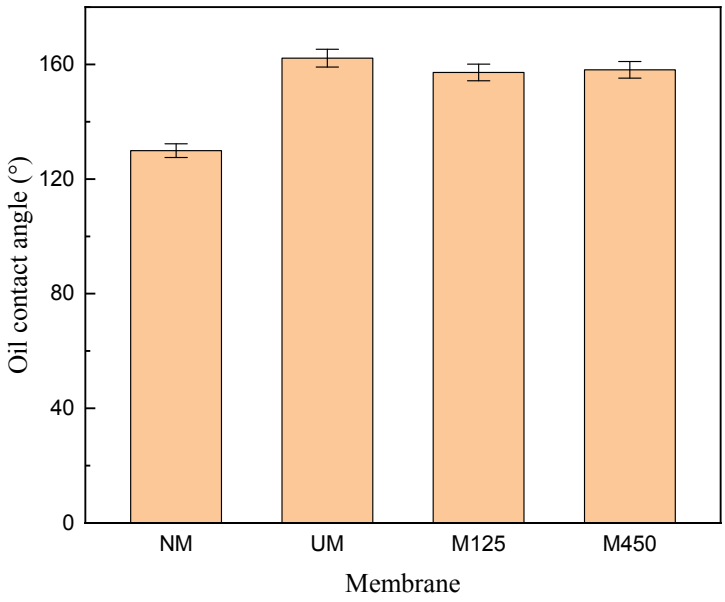

Fig. S7. Oil contact angles under water of the membranes.

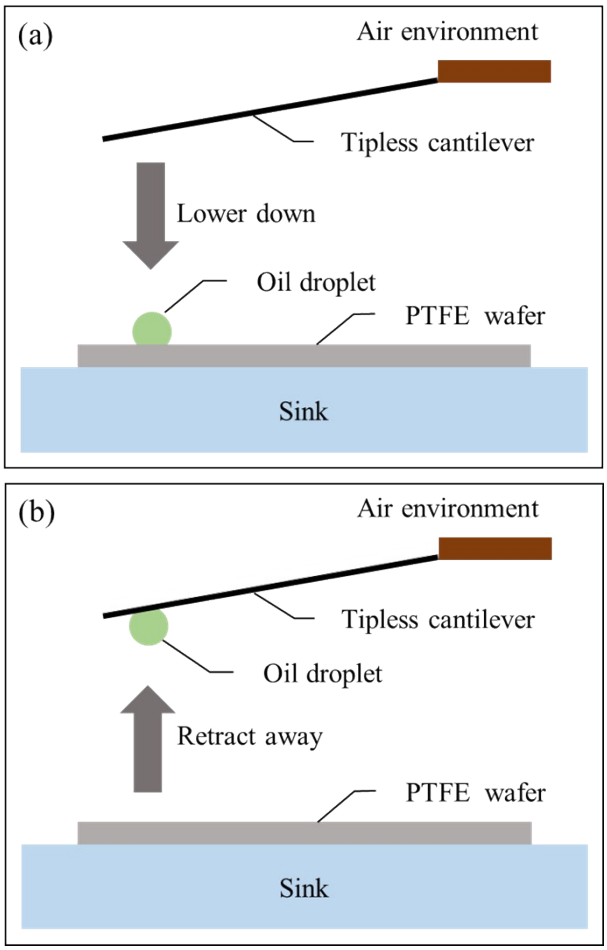

Fig. S8. Schematic illustration of the AFM probe modification by an corn oil droplet. (a) The positioning and lowering of tipless cantilever onto an oil droplet. (b) The retracting of cantilever with an attached oil droplet at the end.

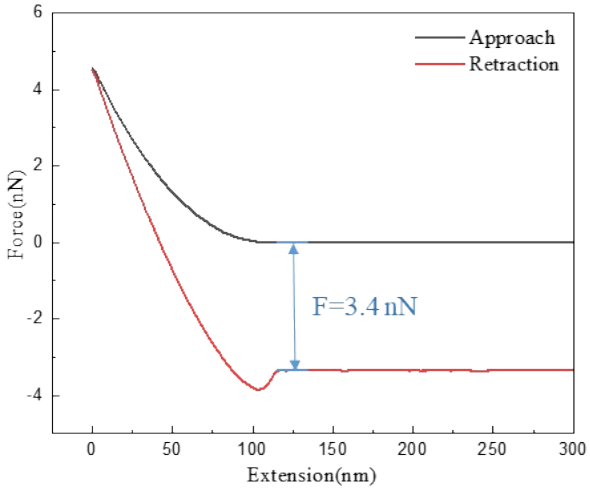

Fig. S9. Force-extension curves of the probe modification.

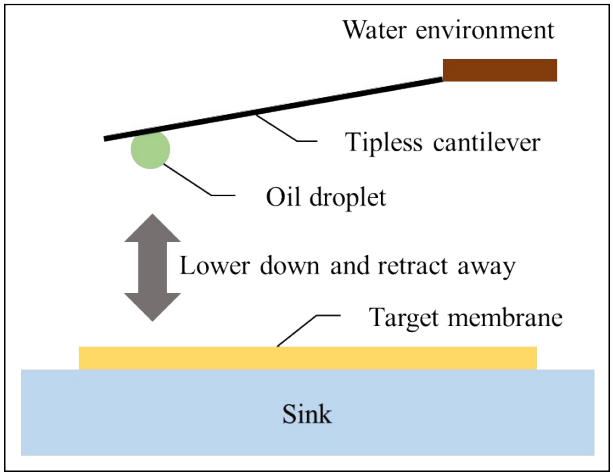

Fig. S10. Schematic illustration of the AFM measurement of adhesion force between an oil droplet and the membrane surface with the modified probe.

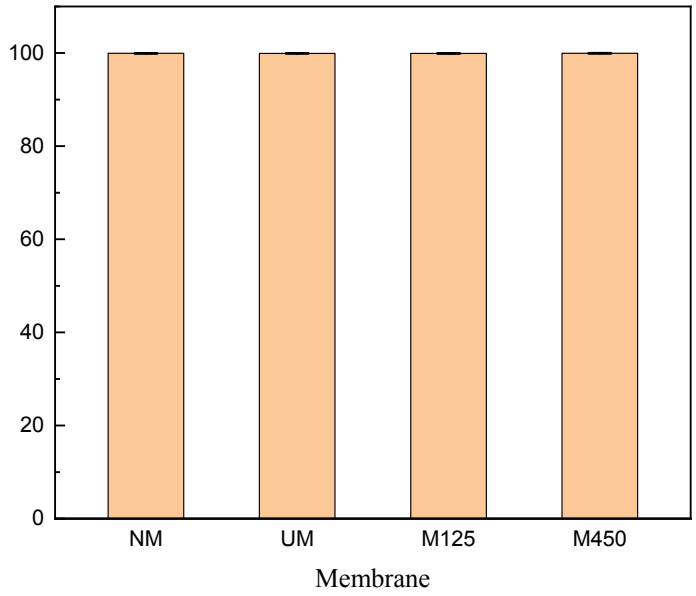

Fig. S11. Rejections of the membranes for oil.

Table S3. Rejections of the membranes for oil in the 6-cycle ultrafiltration experiment.

	Cycle 1	Cycle 2	Cycle 3	Cycle 4	Cycle 5	Cycle 6
NM	99.98	99.96	99.93	99.96	99.97	99.90
UM	99.92	99.96	99.95	99.98	99.97	99.96
M125	99.90	99.96	99.98	99.92	99.93	99.93
M450	99.96	99.94	100.00	99.93	99.97	99.96

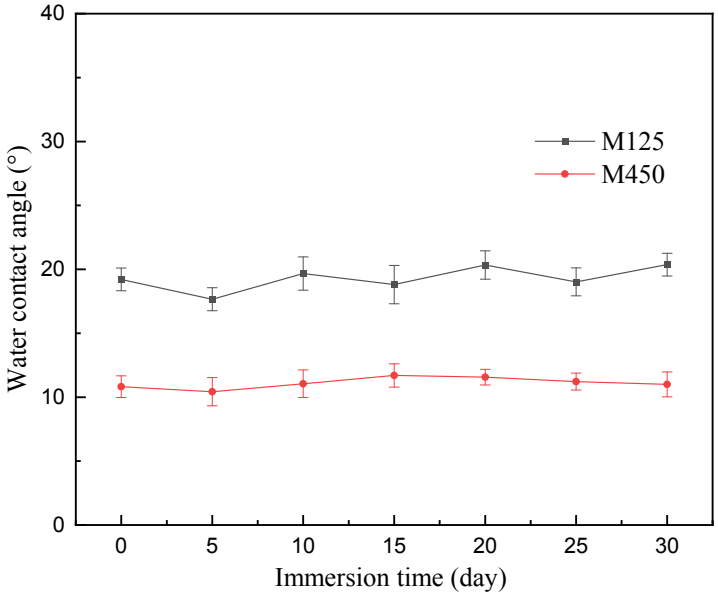

Fig. S12. The water contact angles of M125 and M450 membranes after water dropping 60 s in the scouring experiments. The scouring experiments were carried out in the filtration cell with the stirring speed of 400 rpm and no pressure.

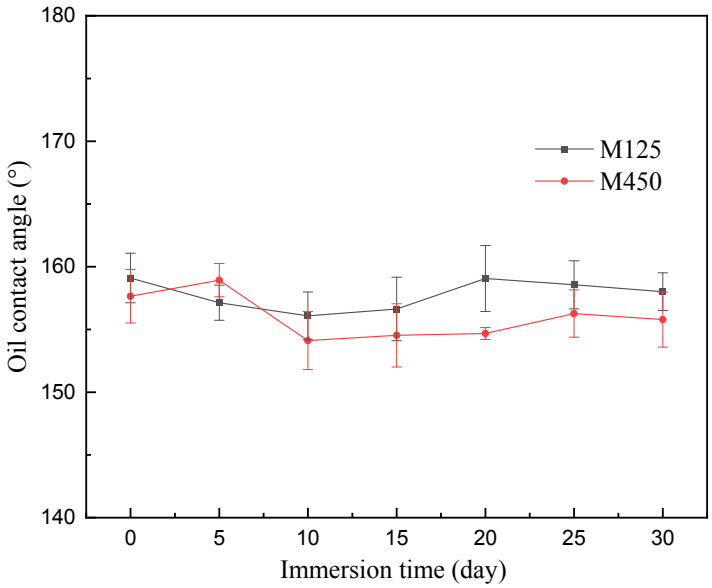

Fig. S13. The oil contact angles of M125 and M450 membranes in the scouring experiments.

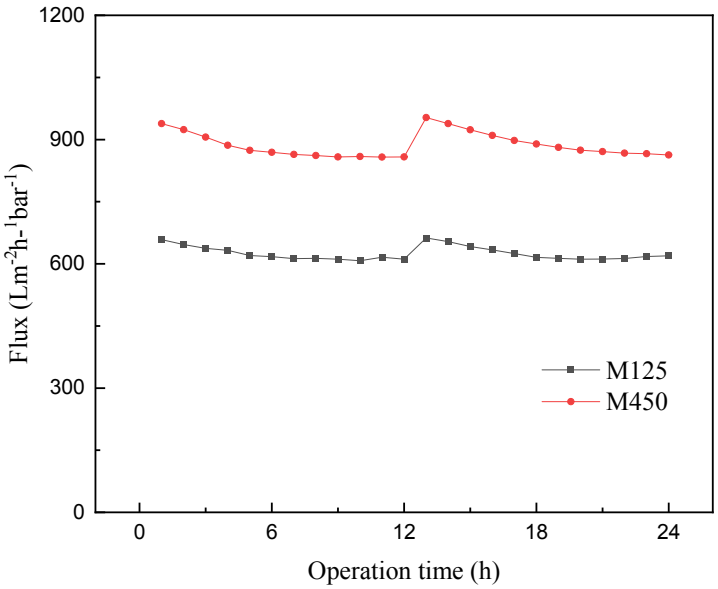

Fig. S14. Operation time-dependent membrane fluxes in the continuous cross-flow experiment. The feed was oil-water emulsion with the average oil droplet size of 420 nm. The water flow rate on the membrane surface was about 0.41 m/s and transmembrane pressure was 1.0 bar. The membrane was hydraulic rinsed for 10 min after 12 h.

Table S4. Permeability and antifouling performance comparison of emulsified oil separation membranes in this study and reported in recent 10 years.

Modification type	Composition	Basic flux ($Lm^{-2}h^{-1}bar^{-1}$)	Separating flux ($Lm^{-2}h^{-1}bar^{-1}$)	FDR (%)	FRR (%)	Flux retention rate (%)
Hydrophilic and LSE	PES/Pluronic F127/PHFMA (M125)	800	730	<9.8	>97.6	>94.5 in 6 cycles
Hydrophilic and LSE	PES/Pluronic F127/PHFMA (M450)	1000	770	<23.5	>92.2	>90.5 in 6 cycles
Hydrophilic and LSE	PVDF/PFSA/PEI-GO[1]	410	375	<8.5	>97.5	>93.0 in 3 cycles
Hydrophilic and LSE	PVDF/PHFBM-PEGMA-PMTAC[2]	190	178	<6.3	>99.9	>85.0 in 3 cycles
Hydrophilic and LSE	PES/PEGMA/TFOA[3]	85	71	<16.8	>99.7	>95.0 in 3 cycles
Hydrophilic and LSE	PVDF-g-PTA/TiO_2[4]	210	206	<2.0	>99.9	/
Hydrophilic and LSE	CA-g-P(HFBM-PEGMA)[5]	75	72	<3.4	>99.9	/
Single hydrophilic	PVDF/TA/DEDAPS[6]	4750	720	<85.0	>98.0	>85.5 in 6 cycles
Single hydrophilic	PAA-g-PVDF/Cu^{2+}/alginate[7]	1600	520	<66.4	>88.3	>86.0 in 3 cycles
Single hydrophilic	PVDF-g-ZNG[8]	2300	1250	<54.5	>99.0	>95.0 in 3 cycles
Single hydrophilic	Hydrolyzed PAN[9]	2600	500	<80.7	>80.0	>67.3 in 3 cycles
Single hydrophilic	Fabric peeled PVDF[10]	10600	2100	<80.0	>99.0	>99.0 in 20 cycles

1. Y. Hao, L. Zhou, Y. Su and Z. Jiang, *Sep. Purif. Technol.*, 2020, **234**.
2. K. Gao, Y. Su, L. Zhou, M. He, R. Zhang, Y. Liu and Z. Jiang, *J. Membr. Sci.*, 2018, **548**, 621-631.
3. G. Zhang, J. Jiang, Q. Zhang, X. Zhan and F. Chen, *AIChE J.*, 2017, **63**, 739-750.
4. X. Zhao, Y. Su, J. Cao, Y. Li, R. Zhang, Y. Liu and Z. Jiang, *J. Mater. Chem. A*, 2015, **3**, 7287-7295.
5. W. Chen, Y. Su, J. Peng, Y. Dong, X. Zhao and Z. Jiang, *Adv. Funct. Mater.*, 2011, **21**, 191-198.
6. Y. Sun, Y. Zong, N. Yang, N. Zhang, B. Jiang, L. Zhang and X. Xiao, *Sep. Purif. Technol.*, 2020, **234**.
7. S. Gao, Y. Zhu, J. Wang, F. Zhang, J. Li and J. Jin, *Adv. Funct. Mater.*, 2018, **28**.
8. Y. Zhu, J. Wang, F. Zhang, S. Gao, A. Wang, W. Fang and J. Jin, *Adv. Funct. Mater.*, 2018, **28**.
9. F. Zhang, S. Gao, Y. Zhu and J. Jin, *J. Membr. Sci.*, 2016, **513**, 67-73.
10. M. Tao, L. Xue, F. Liu and L. Jiang, *Adv. Mater.*, 2014, **26**, 2943-2948.